J Mater Sci (2007) 42:6004–6010
DOI 10.1007/s10853-006-1128-y

Thermoelectric properties of the welded Cu/$Bi_{0.88}$ $Sb_{0.12}$ /Cu composites in the temperature region from 193 K to 298 K

Hirotaka Odahara · Satoru Hiki · Osamu Yamashita · Sunao Sugihara

Received: 31 March 2006 / Accepted: 10 October 2006 / Published online: 6 April 2007

Abstract The resultant thermoelectric properties of Cu/T/Cu composites welded with T = $Bi_{0.88}Sb_{0.12}$ alloy were measured in the temperature range from T = 193 K to 298 K and compared with those calculated as a function of x by treating these composites as an electrical and thermal circuit, where x is the ratio of thickness of Bi–Sb alloy to the interval between two thermocouples. Consequently, the resultant electrical resistivities ρ of composites coincided closely with the calculated ρ values as a function of x, while the resultant Seebeck coefficients α were enhanced significantly in the range from x=0.076 to 0.61. In the x range from 0.16 to 1.0, the x-dependence of the resultant thermoelectric power factor P was found to be explained roughly at every temperature by the simple model proposed here when an enhancement factor in α was taken into the calculation. However, the maximum resultant P appeared at a small x of 0.076. The resultant P at x = 0.076 increases with a decrease of T and reached a surprisingly great value of 128.3 mW/K^2 m at 193 K, which is 15.5 times larger than 8.29 mW/K^2 m obtained for $Bi_{0.88}Sb_{0.12}$ alloy. On the other hand, its resultant ZT also increases monotonically with a decrease of T and has a great value of 0.54 at 193 K, which is 31% higher than 0.41 at 193 K for Bi–Sb alloy. The significant enhancement in the resultants P and ZT at low temperatures is owing predominantly to the increase in α due to the boundary effect.

Introduction

In recent years there has been renewed interest in finding new materials and structures for use in highly efficient cooling and energy conversion systems [1, 2]. This interest has been stimulated in considerable part by the opportunities that quantum well and quantum wire superlattices [3–5] might result in thermoelectric materials with high power factors $P = \alpha^2/\rho$, where α is the Seebeck coefficient and ρ is the electrical resistivity. The thermoelectric power factor P is given in terms of the material's electrical transport properties, and it enters the thermoelectric figure of merit $Z = P/\kappa$, where κ is the total thermal conductivity which contains both lattice and electronic contributions. Thus, P provides a measure of the quality of a material for cooling [6].

Recently, the resultant thermoelectric power factor P of two-component composite was calculated by Bergman and Fel [7], who predicted theoretically that the resultant P can be greater than the power factors of two different pure components at an optimum volume fraction, but the resultant ZT never exceeds those of two different pure components, at least when the resultant α across the boundary is not enhanced. Indeed, such an enhancement in P has been observed in various types of macroscopic composites in which a thermoelectric material is sandwiched between two metals [8–12]. When there is some enhancement in α, however, the resultant ZT of composites was also increased significantly [9, 11].

When a semiconductor is kept in contact with a metal or a semiconductor with different types of conduction, a potential barrier generally occurs at their interfaces. Tauc [13]

H. Odahara · O. Yamashita (✉)
Faculty of Engineering, Ehime University, Bunkyocho, Matsuyama 790-8577, Japan
e-mail: yamashio567@yahoo.co.jp

S. Hiki · S. Sugihara
Department of Materials Science and Ceramic Technology, Shonan Institute of Technology, 1-1-25, Tsujido Nishikaigan, Fujisawa 251-8511, Japan

indicated theoretically about 50 years ago that when such a barrier was accompanied by a sufficiently great temperature drop, the additional barrier thermo-emf appears as a result of the separation of non-equilibrium carriers at the interface. The appearance of the barrier thermo-emf was indeed observed in the p-n junctions by illuminating them with infrared light pulse from a laser [14]. Most recently, similar phenomenon was also observed as an enhancement in the resultant α even in macroscopic thermoelectric composites corresponding to the metal–semiconductor junction, in which a thermoelectric semiconductor is sandwiched between two metals [8–11]. For example, the resultant maximum α of the n-type Cu/Bi–Sb/Cu composite welded with $Bi_{0.88}Sb_{0.12}$ alloy was –110 μV/K, which is 29% higher in absolute value than –85 μV/K of Bi–Sb alloy [9]. Similarly, the resultant maximum α of the n-type Cu/Bi/Cu composite welded with pure Bi was 21% higher in absolute value than –70 μV/K of Bi.[10] In addition, the maximum α values of welded p- and n-type Cu/Bi-Te/Cu composites were approximately 32% and 30% higher in absolute value than 202 and –205 μV/K of the intrinsic Bi–Te compounds [11]. Such increase in α was owing to the contribution from the additional barrier thermo-emf to the overall thermo-emf, and it is referred to as the boundary effect. Indeed, the increase in α resulted in the significant enhancement in the resultants P and ZT of composites [8–11].

Generally, the barrier thermo-emf occurs in the forward-bias direction (with a plus sign in the p-type region and a minus sign in the n-type region) or in the reverse-bias direction, depending on the position of the temperature gradient and the physical properties of the interface [14]. The barrier thermo-emf occurs in the forward-bias direction, at least in the present composites. Most recently, it was clarified by us that the resultant α across the boundary of Cu/Bi–Te/Cu composites is enhanced strongly in the Bi–Te region near the boundary, not at the boundary between Bi–Te material and copper [15]. The place where the Seebeck coefficient is enhanced most strongly was several tens micrometers distant from the surface of Bi–Te materials touched with the copper plate [15].

In this paper, the dependence of the resultant power factor P on the relative thickness of Bi–Sb alloy was investigated at low temperatures below room temperature for macroscopic Cu/Bi–Sb/Cu composites. The resultant P of a composite was calculated as a function of relative thickness of Bi–Sb alloy by treating it as an electrical and thermal circuit and was compared with the experimental P.

The purpose of this paper is to investigate to what degree the resultants α, P and ZT of the welded Cu/Bi–Sb/Cu composites are enhanced by the boundary effect at low temperatures below room temperature, as compared with their experimental values at room temperature.

Calculations and experiments

Calculations of electrical resistivity, Seebeck coefficient and power factor of a composite device

Let us consider a thermoelectric composite with a sandwich structure (A/B/A) in which a disc of the thermoelectric material B is sandwiched between two cylinders composed of the metallic material A, as shown in Fig. 1. Here, we calculate the resultants P and ZT for a composite by treating it as an electrical and thermal circuit, in which the direction of the temperature gradient is along the cylindrical axis [8, 9]. The materials A and B have the same cross-sectional area S and two different thicknesses t_A and t_B, respectively. It was assumed here that the scattering of carriers and phonons never occurs at the interface between a disc and two cylinders. When the electrical resistivities of the materials A and B are ρ_A and ρ_B and the total thickness is t, the total electrical resistivity ρ of a composite is expressed as

$$\rho = \frac{1}{t}(2\rho_A t_A + \rho_B t_B). \quad (1)$$

Here if we suppose $t_A = t(1-x)/2$ and $t_B = tx$, the resultant ρ can be rewritten as a function of x as

$$\rho(x) = \rho_B\{x + b(1-x)\}, \quad (2)$$

where $b = \rho_A/\rho_B$. Similarly, the total thermal conductivity κ of a composite is expressed as a function of x as

$$\frac{1}{\kappa(x)} = \frac{(1-x)}{\kappa} + \frac{x}{\kappa_B} = \frac{1}{\kappa_B}\left\{x + \frac{(1-x)}{c}\right\} \quad (3)$$

where $c = \kappa_A/\kappa_B$. For a given temperature difference ΔT, the temperature difference generated in a thermoelectric

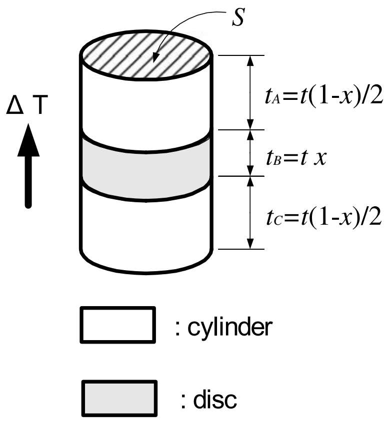

Fig. 1 Thermoelectric composite with a sandwich structure (A/B/A) in which a disc of thermoelectric material B is sandwiched between two cylindrical materials A. The direction of the temperature gradient is along the cylindrical axis of the composite

material should be proportional to thickness but inversely proportional to thermal conductivity, at least for a thin composite. When the thermal conductivities of the materials A and B are $\kappa_A$and κ_B, therefore, the ratio of ΔT_A to ΔT_B is expressed as

$$\frac{\Delta T_A}{\Delta T_B} = \frac{t_A \kappa_B}{t_B \kappa_A} = \frac{(1-x)}{2cx} \tag{4}$$

where $c = \kappa_A/\kappa_B$. The total temperature difference ΔT between both ends of a composite is given by

$$\Delta T = 2\Delta T_A + \Delta T_B. \tag{5}$$

By substituting Eq. 4 into Eq. 5, the ratio of thermal difference ΔT_B generated in a sandwiched material B to the total thermal difference ΔT is expressed as

$$\frac{\Delta T_B}{\Delta_T} = \frac{cx}{(1-x)+cx}. \tag{6}$$

When the Seebeck coefficients of the materials A and B are α_A and α_B, the total thermal voltage ΔV generated by ΔT_A and ΔT_B is written as

$$\Delta V = \Delta T_A \alpha_A + \Delta T_B \alpha_B. \tag{7}$$

Therefore, the overall Seebeck coefficient α is expressed as a function of x as

$$\alpha(x) = \frac{\Delta V}{\Delta T} = \alpha_B \frac{(1-x)a+cx}{(1-x)+cx} \tag{8}$$

using Eqs. 4–7, where $a = \alpha_A/\alpha_B$. In general, the thermoelectric power factor P and thermoelectric figure of merit Z are given by

$$P = \alpha^2/\rho \tag{9}$$

and

$$Z = P/\kappa, \tag{10}$$

respectively. Substituting Eqs. 2, 3 and 8 into Eqs.9 and 10, the resultants P and Z are expressed as a function of x using P_B and κ_B of the thermoelectric material B as

$$P(x) = P_B \left\{ \frac{(1-x)a+cx}{(1-x)+cx} \right\}^2 \frac{1}{\{x+b(1-x)\}}, \tag{11}$$

and

$$Z(x) = \frac{P(x)}{\kappa_B} \left\{ x + \frac{(1-x)}{c} \right\} \tag{12}$$

respectively, where $P_B = \alpha_B^2/\rho_B$. Of course, $P(x)$ and $Z(x)$ reduce to $P = P_B$ and $Z = P_B/\kappa_B$ if $x = 1$ and to $P = P_A$ and $Z = P_A/\kappa_A$ if $x = 0$. As described above, $P(x)$ has a local maximum at an optimum x for an optimum combination of a, b and c, but $Z(x)$ cannot exceed the largest among the component materials, as long as the resultant α of a composite cannot be increased [7].

Sample preparation and measurements

The Cu/T/Cu(T = $Bi_{0.88}Sb_{0.12}$) composites were prepared by the welding method, using Cu of 99.9% and Bi–Sb alloy of 99.99%, which have cylindrical shapes with a diameter slightly smaller than 5 mm. The cylindrical ingots of Bi–Sb alloy were prepared by melting in an evacuated glass tube of an inner diameter slightly smaller than 5 mm by an induction heating to make a homogeneous melt without segregation. The thickness of coppers was determined so that Bi–Sb alloy sandwiched between two coppers has various thicknesses but the total length of composites becomes 20 mm. After both end surfaces of all cylindrical coppers were polished mechanically by the lapping method to make flat the welded surface, a set of two cylindrical coppers and Bi–Sb alloy was put in a glass tube of an inner diameter φ 5 mm so that Bi–Sb alloy is sandwiched between two coppers in a glass tube. Since $Bi_{0.88}Sb_{0.12}$ alloy has a very low melting point of 598 K [16], the alloy was first melted between two coppers in a glass tube by an induction heating. While Bi–Sb alloy is melted, two cylindrical coppers of both ends were compacted at a constant force of 2 N using two nickel rods, as shown in Fig. 2. After a welded cylinder was naturally cooled to room temperature, it was ejected from a glass tube using an iron rod. A representative photograph of the present composite is shown in Fig. 3a. The thickness t_B of Bi–Sb alloy

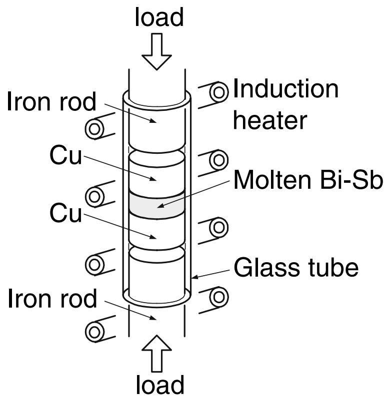

Fig. 2 Fabrication method of composites welded with $Bi_{0.88}Sb_{0.12}$ alloy

was measured by polishing the surface along the cylindrical axis of a welded composite, so that the boundary between copper and Bi–Sb alloy becomes clear, as shown in Fig. 3b. After polishing, no crack and no exfoliation were detected at the boundaries of all composites. Then the average grain sizes of Bi–Sb alloy were approximately 100 μm, which remained almost unchanged before and after welding.

All of the composites were subjected to Seebeck coefficient and electrical resistivity measurements (Sinku-Riko, Inc., Model ZEM-1). The Seebeck coefficient α was measured by the conventional technique, using two alumel–chromel thermocouples set at an interval of 8 mm, in the temperature range from 193 K to 298 K with the temperature difference of about 5 K. The composites were then adjusted so that two coppers of both ends have the same length between two thermocouples. The electrical resistivity ρ was measured concurrently by the four-probe method. All of these measurements were performed along the cylindrical axis. The experimental results of pure Cu and $Bi_{0.88}Sb_{0.12}$ at 193, 243 and 298 K are listed in Table 1, in which κ values are taken from refs. 17 and 18. The thermoelectric properties of α and ρ were measured within accuracies of 3 and 2%, respectively. The resultant accuracy of the resultants P and ZT was about 13%, at least when the experimental error in the resultant κ is not taken into account.

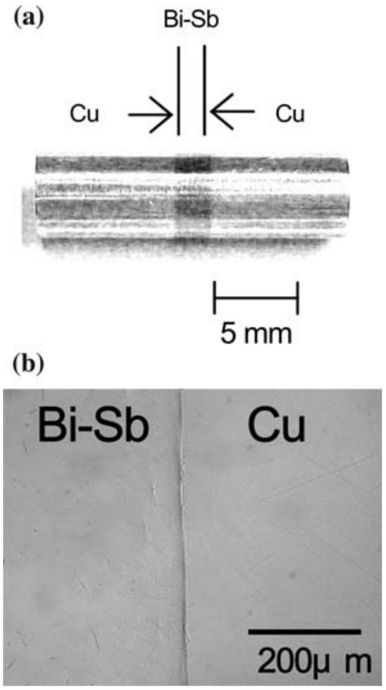

Fig. 3 A photograph of welded Cu/Bi–Sb/Cu composite and a microphotograph of the boundary of a welded composite

Results and discussion

Dependence of the resultants ρ and α on relative thickness x of $Bi_{0.88}Sb_{0.12}$

The resultants ρ and α of Cu/Bi–Sb/Cu composites with different x values were measured in the temperature range from 193 K to 298 K, where x is the ratio of thickness of Bi–Sb alloy to an interval of 8 mm. The measured ρ value at 298 K (see Table 1) of $Bi_{0.88}Sb_{0.12}$ alloy is 10.4% higher than the value obtained by Yim and Amith [19]. However, the experimental α values at 193, 243 and 298 K (see Table 1) of $Bi_{0.88}Sb_{0.12}$ alloy coincided closely with those calculated as the mean value using the equation $\alpha = (\alpha_{33} + 2\alpha_{11})/3$, where α_{33} and α_{11} were Seebeck coefficients measured along the trigonal and binary directions of single-crystal $Bi_{0.88}Sb_{0.12}$ [19]. Since α of single-crystal $Bi_{0.88}Sb_{0.12}$ alloy has little anisotropy, however, α of $Bi_{0.88}Sb_{0.12}$ alloy hardly depends on whether the welded Bi–Sb alloy is an isotropic polycrystalline.

As shown in Fig. 4, the observed ρ values at 193, 243 and 298 K of Cu/Bi–Sb/Cu composites increase linearly with an increase of x and fall almost on the solid curves $\rho(x)$ calculated from Eq. 2 using the experimental values, as listed in Tables 1 and 2. In contrast, the observed α values increase abruptly with an increase of x and tend to have a gentle local maximum at $x = 0.61$, except for an α value at $x = 0.076$. The local maximum α at $x = 0.61$ is 18–20% higher in absolute value than the solid curve α (x) calculated from Eq. 8 using the experimental values at every temperature, as listed in Tables 1 and 2. The degree of increase in α at $x = 0.61$ was found to have only a little dependence on temperature. In the x range from 0.16 to 1.0, the x-dependence of the resultant α agreed well with the dashed curves obtained by multiplying the dotted curves α (x) obtained using both the experimental values at each temperature and c values (see Fig. 4) smaller than $\kappa_{\mathrm{Cu}}/\kappa_{\mathrm{Bi-Sb}}$ by an enhancement factor of $\{1 + 0.55x(1-x)^{0.5}\}$. Interestingly, however, the resultant α at $x = 0.076$ depends strongly on temperature, unlike α in the x region above 0.16. The resultants α at 298, 243 and 193 K are 6%, 28% and 36% higher in absolute value than the solid curves, respectively, as shown in Fig. 4. The enhancement in the resultant α at small $x(\approx 0.15)$ has also been observed at 298 K in Cu/Bi/Ni composites [8]. These enhancement in α at small x is consistent with the previous result that the resultant α of composites is increased significantly at the shallow of thermoelectric materials [15]. The disagreement between the observed and calculated α values at small x, therefore, results from the contribution from the additional barrier thermo-emf to the overall thermo-emf. The degree of disagreement tends to become larger at lower temperatures, as already described.

Table 1 Electrical resistivities and Seebeck coefficients measured at 193, 243 and 298 K for pure Cu and $Bi_{0.88}Sb_{0.12}$ cylindrical rods with a length of 20 mm and a diameter of φ 5 mm

	Cu			$Bi_{0.88}Sb_{0.12}$		
	193 K	243 K	298 K	193 K	243 K	298 K
Electrical resistivity ρ ($\mu\ \Omega$ m)	0.0100	0.0134	0.0171	1.27	1.48	1.70
Seebeck coefficient α (μ V/K)	1.3	1.7	1.9	–103	–113	–85.1
Thermal conductivity κ (W/mK)	415[a]	407[a]	401[a]	3.87[b]	4.18[b]	4.41[b]
Power factor P (mW/K^{2}m)	0.17	0.22	0.21	11.5	8.63	4.25
Figure of merit ZT	6.1×10^{-4}	1.3×10^{-4}	1.6×10^{-4}	0.41	0.36	0.29

[a] Ref. 17, [b]Ref. 18

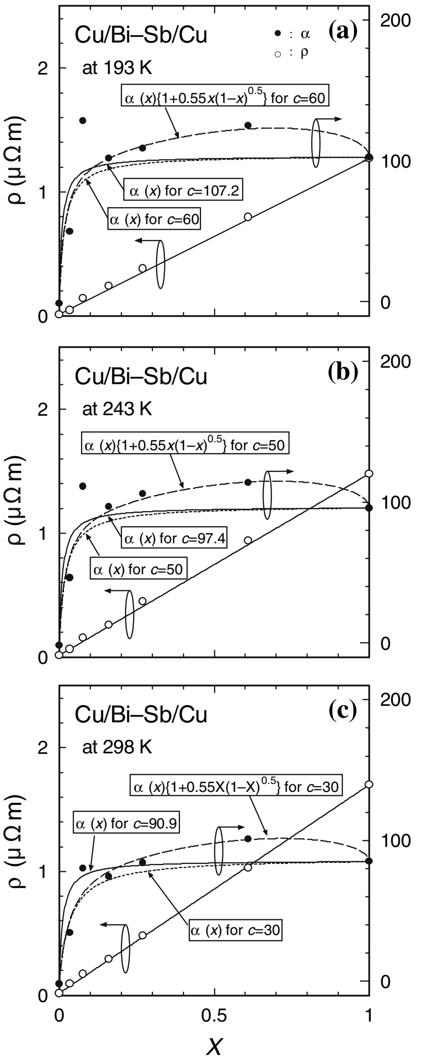

Fig. 4 Resultants ρ and α measured at 193, 243 and 298 K as a function of x for welded Cu/Bi–Sb/Cu composites. The solid curves of ρ (x) and α (x) are calculated from Eqs 2 and 8 for Cu/Bi–Sb/Cu composites, respectively, where the experimental values and parameters used here are listed in Tables 1 and 2. The dashed curves are obtained by multiplying the dashed curves α (x) calculated using smaller c among two different c values by a factor of $\{1 + 0.55x(1 - x)^{0.5}\}$, so as to reproduce well the observed α values

Therefore, the boundary effect is thus found to become stronger at lower temperatures. The mechanism for the enhancement in α due to the boundary effect would thus differ with the relative thickness x of thermoelectric materials. If so, the optimum interface condition fitted to increase in the resultant α might also differ with x. However, it would be very difficult technically to reproduce the optimum interface at the boundary by controlling the welding process.

As evident from the fact that α of $Bi_{0.88}Sb_{0.12}$ has little anisotropy, it is clear that the enhancement in α after welding has nothing to do with the degree of alignment of the c axis of welded $Bi_{0.88}Sb_{0.12}$ alloy. Therefore, such significant enhancement in the resultant α across the boundary is owing to the contribution from the additional barrier thermo-emf generated near the boundary which has the same sign as those of the intrinsic Bi–Sb alloy, as in the case of various types of composites [8–11].

Dependence of the resultants P and ZT on relative thickness x of $Bi_{0.88}Sb_{0.12}$

The observed P values at 193, 243 and 298 K of Cu/Bi–Sb/Cu composites were plotted as a function of x in Fig. 5 and compared with the theoretical curves calculated using the experimental values at each temperature; the solid and dotted curves were calculated by substituting two different c values into Eq. 11 and the dashed curve is obtained by multiplying α (x) calculated using smaller c among two different c values by an enhancement factor of $\{1 + 0.55x(1 - x)^{0.5}\}$. The observed P increases abruptly

Table 2 Parameters a, b and c estimated at 193, 243 and 298 K for the welded Cu/Bi–Sb/Cu composite

Parameter	Temperature (K)		
	193	243	298
a	–0.0107	–0.0150	–0.0223
b	0.00787	0.00905	0.0101
c	107.2	97.4	90.9

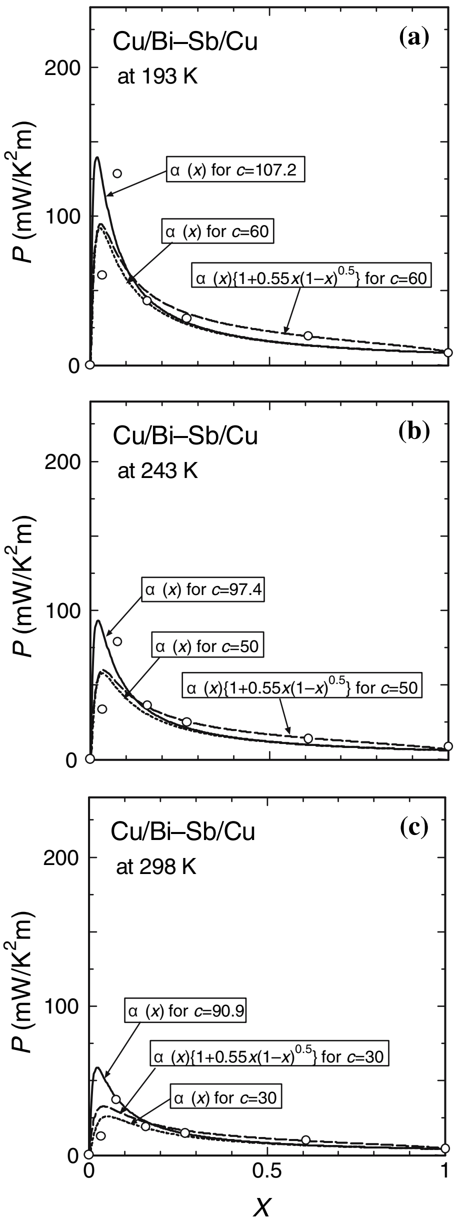

Fig. 5 Resultant P measured at 193, 243 and 298 K as a function of x for welded Cu/Bi–Sb/Cu composites. The solid curves denote P values calculated from Eq. 11 using the experimental values and parameters listed in Tables 1 and 2. The dotted curves are calculated from Eq. 11 using smaller c among two different c values and the dashed ones are obtained by multiplying the dotted curves α (x) by a factor of $\{1 + 0.55x(1 - x)^{0.5}\}$

with an increase of x, reaches a local maximum at $x = 0.076$ and tends to decrease slowly with further increase of x. As a whole, the x-dependence of the resultant P is also found to be explained well at every temperature in the x region above 0.16 by the simple model proposed here, at least when an enhancement factor in α was taken into account. Below $x = 0.10$, however, the observed P values do not agree with all calculated curves, like the resultant α, except for $x = 0.076$ at 298 K. The local maximum of P at $x = 0.076$ increases with a decrease of temperature and reached a surprisingly great value of 28.3 mW/K^2 m at 193 K, which is 15.5 times larger than 8.29 mW/K^2 m obtained for $Bi_{0.88}Sb_{0.12}$ alloy and is about 45% higher than 88.3 mW/K^2 m obtained at 298 K for the n-type Ag/Bi–Te/Ag composites welded with pure Bi [12].

The resultant P was plotted as a function of T for the welded Cu/Bi–Sb/Cu composite with $x = 0.076$ and for Bi–Sb alloy corresponding to $x = 0$ in Fig. 6a. In the figure, the dashed curves below $T = 193$ K denote the resultant P expected for $x = 0.076$. The dashed curve estimated from Eq. 11 using both $x = 0.017$ giving a local maximum of P and the experimental α, ρ and κ values measured at 80, 114, 156 and 193 K by Yim and Amith [19] was normalized to coincide with the experimental P at 193 K, because the observed P at $x = 0.076$ is rather close to the P value calculated as $x = 0.017$ using the experimental values (listed in Tables 1, 2) at 193 K. As shown in Fig. 6a, so calculated P increases monotonically with further decrease of T and is expected to reach an extremely great value of

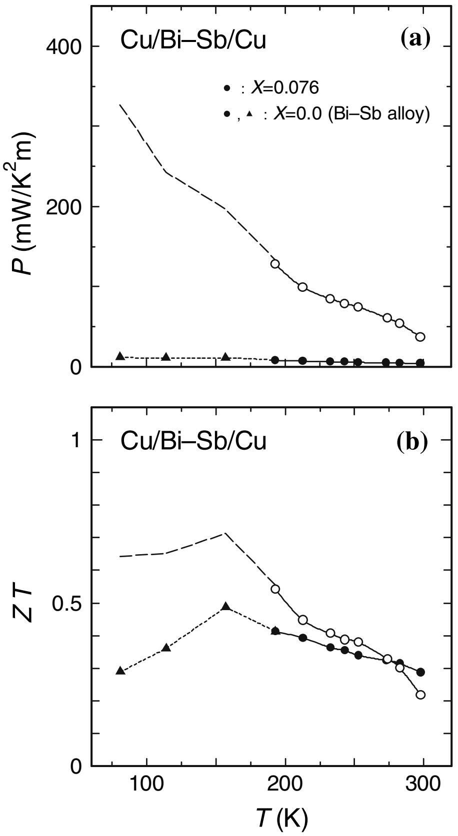

Fig. 6 Resultants P and ZT as a function of T for a welded Cu/Bi–Sb/Cu composite with $x = 0.076$ and for Bi–Sb alloy corresponding to $x = 0$. Open and full circles denote our experimental values and full triangles do the experimental values obtained by Yim and Amith [19]. The dashed curves below $T = 193$ K denote the resultants P and ZT expected for $x = 0.076$ and the dotted one does the experimental P and ZT [19] for Bi–Sb alloy

327 mW/K^2 m at 80 K, which is 2.55 times as large as 128.3 mW/K^2 m measured at 193 K and reaches 27.5 times larger than 11.9 mW/K^2 m of $Bi_{0.88}Sb_{0.12}$ alloy at 80 K. The resultant *P* of the welded Cu/Bi–Sb/Cu composite was found to be enhanced markedly with a decrease of *T*, as compared to that of Bi–Sb alloy. It is owing to the increase in α with a decrease of *T*.

The resultant *ZT* calculated from Eq. 12 was plotted as a function of *T* for the welded Cu/Bi–Sb/Cu composite with $x = 0.076$ and for Bi–Sb alloy in Fig. 6b. The dashed curve below $T = 193$ K denote the resultant *ZT* expected for $x = 0.076$. The dashed curve estimated using Eq. 12 was also normalized to coincide with the experimental *ZT* at 193 K, using the same method used in drawing the dashed curve of *P*. As shown in Fig. 6b, so estimated *ZT* increases monotonically with a decrease of *T*, has a local maximum of 0.71 at 157 K and tends to decrease with further decrease of *T*. This temperature dependence of *ZT* is very similar to that of Bi–Sb alloy. The observed *ZT* at $x = 0.076$ reached a great value of 0.54 at 193 K, which is 31% higher than 0.41 at 193 K for Bi–Sb alloy. The resultant *ZT* of a composite with an optimum thickness of Bi–Sb alloy was expected to become much higher than that of Bi–Sb alloy at lower temperatures below 200 K. It is also owing to the enhancement in α due to the boundary effect, like the resultant *P*.

It is thus found that the welded Cu/Bi–Sb/Cu composite with an optimum thickness of Bi–Sb alloy is fitted for a thermoelectric generator operating at low temperatures.

Summary and conclusion

The resultant thermoelectric properties of Cu/T/Cu composites welded with $T = Bi_{0.88}Sb_{0.12}$ alloy were measured in the temperature range from $T = 193$ K to 298 K and compared with those calculated as a function of *x* by treating these composites as an electrical and thermal circuit, where *x* is the ratio of thickness of Bi–Sb alloy to the interval between two thermocouples. Consequently, the resultant electrical resistivities ρ of composites coincided closely with the calculated ρ values as a function of *x*, while the resultant Seebeck coefficients α across the boundary were enhanced significantly in the range from $x = 0.076$ to 0.61, as compared with the solid curves, owing to the boundary effect. At $x = 0.61$, the degree of enhancement in α has little dependence on temperature and was 18–20%, while at $x = 0.076$, it was increased from 6% to 36% when the temperature was lowered from 298 K to 193 K. In the *x* region from 0.16 to 1.0, the *x*-dependence of the resultant *P* was explained roughly at every temperature by the simple model proposed here when an enhancement factor in α was taken into the calculation, while in the *x* region below 0.10, there was a significant disagreement between the observed and calculated *P* values. The resultant *P* at $x = 0.076$ becomes higher than the calculated (solid) curve as *T* is decreased, owing to a significant increase in the resultant α due to the boundary effect at lower temperatures. The resultant *P* at $x = 0.076$ reached a surprisingly great value of 28.3 mW/K^2 m at 193 K, which is 15.5 times larger than 8.29 mW/K^2 m obtained for $Bi_{0.88}Sb_{0.12}$ alloy and is about 45% higher than 88.3 mW/K^2 m obtained at 298 K for the n-type Ag/Bi–Te/Ag composites welded with pure Bi. On the other hand, its resultant *ZT* increases monotonically with a decrease of *T*, has a local maximum of 0.71 at 157 K and tends to decrease with further decrease of *T*. The observed *ZT* at $x = 0.076$ reached a great value of 0.54 at 193 K, which is 31% higher than 0.41 at 193 K for Bi–Sb alloy. The resultants *P* and *ZT* of Cu/Bi–Sb/Cu composite with an optimum thickness of Bi–Sb alloy were expected to become much higher than those of Bi–Sb alloy at lower temperatures below 200 K.

The increase in the resultants *P* and *ZT* is owing predominantly to a significant enhancement in α due to the boundary effect. The boundary effect on the resultant α across the interface was found to become stronger at lower temperatures. The welded Cu/Bi–Sb/Cu composite with an optimum thickness of Bi–Sb alloy is thus fitted for a thermoelectric generator operating at low temperatures.

References

1. Wood C (1988) Prog Phys 51:459
2. Mahan G, Sales B, Sharp J (1997) Phys Today 50:42
3. Hicks LD, Dresselhaus MS (1993) Phys Rev B 47:12727
4. Hicks LD, Harman TC, Dresselhaus MS (1993) Appl Phys Lett 63:3230
5. Broido DA, Reinecke TL (1995) Appl Phys Lett 67:1170
6. Goldsmid HJ (1964) Thermoelectric refrigeration. Plenum, NewYork
7. Bergman DJ, Fel LG (1999) J Appl Phys 85:8205
8. Odahara H, Yamashita O, Satou K, Tomiyoshi S, Tani J, Kido H (2005) J Appl Phys 97:103722
9. Yamashita O, Satou K, Odahara H, Tomiyoshi S (2005) J Appl Phys 98:073707
10. Yamashita O, Odahara H, Satou K (2005) J Mater Sci 40:1071
11. Yamashita O, Odahara H (2006) J Mater Sci 41:2795
12. Yamashita O, Odahara H, Satou K, Tomiyoshi S (2006) J Mater Sci 41:3097
13. Tauc J (1953) Czechosl J Phys 3:282
14. Balmush II, Dashevsky ZM, Kasiyan AI (1995) Semiconductors 29:937
15. Yamashita O, Odahara H (in press) Appl Phys A
16. Lenoir B, Demouge A, Perrin D, Scherrer H, Scherrer S, Cassart M, Michenaud JP (1995) J Phys Chem Solids 56:99
17. Kittel C (1996) Introduction to solid state physics. John Wiley & Sons, NewYork
18. Lide DR (1964) CRC handbook of chemistry and physics, 84th edn. CRC Press
19. Yim WM, Amith A (1972) Solid State Electrons 15:1141
20. Venkatasubramanian R, Siivola E, Colpitts T, O'quinn B (2001) Nature 413:597